High power and low noise mode-locking operation of Al-quaternary laser diodes

Piotr M. Stolarz, Vincenzo Pusino, Jehan Akbar, Gábor Mezősi, Lianping Hou, A. Catrina Coleman, *Fellow IEEE*, John H. Marsh, *Fellow IEEE*, Anthony E Kelly, and Marc Sorel *Member IEEE*

***Abstract*— We report on the design and experimental evaluation of AlGaInAs/InP multi-quantum-well epi-structures for mode-locked emission at 1.5-μm. We show that mode-locked lasers fabricated on an optimized 3 quantum-well active region with a low optical confinement factor deliver pulses with increased peak power and stability over a much wider biasing range than those fabricated using a standard 5 quantum well design. Sonogram measurements indicate that sub-ps symmetrical pulses with a substantially reduced linear blue chirp are generated up to nearly three times the laser current threshold.**

***Index Terms*—Semiconductor lasers, Mode locked lasers, Pulse measurements, Quantum Well lasers.**

I. Introduction

MODE-LOCKED lasers (MLLs) are effective sources of periodic sequences of coherent optical pulses and constitute a fundamental component in a range of optical communications and spectroscopy applications [1–3]. Passive mode-locking (PML), based on the combination of gain and loss saturation mechanisms resulting in self-sustained pulsed optical output has been demonstrated in many different types of laser systems [4–6]. Amongst the various devices proposed, integrated semiconductor lasers are particularly attractive because of their low cost, high efficiency and short cavity lengths that lead to repetition rates ranging between 40 GHz to 2 THz. However, their operation is usually limited to average output levels of a few tens of milliwatts per facet, due to the bleaching of the saturable absorber at increasing intra-cavity optical intensity, and to pulse energies of a few pJ because of gain saturation. Furthermore, non-linearities such as self-phase modulation (SPM) tend to broaden the pulses in time and frequency, and result in a large increase in jitter.

In this work, we investigate the effect of an optimized epitaxial structure for increasing the pulse energies and improving mode-locking (ML) properties of semiconductor lasers, such as emission stability, timing jitter, pulse width and chirp. The article is organized as follows: Section II illustrates the investigated epitaxial structures, presents an overview of the operational parameters of interest and discusses the modifications introduced. Section III compares the performance of a standard 5 quantum well (QW) epi-layer design and the modified 3 QW design through a detailed experimental characterization of the devices. Finally, Section IV summarizes the results.

Manuscript received XX.

The authors are with the School of Engineering, University of Glasgow, G12 8LT, Glasgow, UK, e-mail: Vincenzo.Pusino@glasgow.ac.uk.

II. Device Design

The laser material used as a reference in this work was a commercially available multi-quantum-well (MQW) InAlGaAs/InP wafer structure with a gain region consisting of five 6 nm thick compressively strained AlGaInAs QWs and six 10 nm thick slightly tensile strained barriers. On each side of the QWs, the core layers are formed by 60 nm graded-index separate confinement heterostructures (GRINSCHs). More detailed description of the epitaxial structure can be found in [7]. The structure has been assessed in great detail over the last few years and showed excellent performance when used for fabricating semiconductor ring lasers (SRLs) [8], distributed feedback (DFB) [9] lasers and narrow linewidth semiconductor MMLs. However, the epitaxial structure was not designed with MLL operation in mind.

The following section will discuss how the epi-layer structure can be improved to deliver high pulse energy, low timing jitter, narrow pulsewidths, stable ML operation over a wide parameter range and low chirp.

A. Pulse Energy

Conventional monolithic semiconductor mode-locked lasers (SMLLs), although compact and low-cost compared to their solid-state and fiber counterparts, typically produce low energy pulses and limited average output powers. The maximum achievable pulse energy is dependent on the gain saturation energy, E_{sat} [10], which is given by the following relation [11]:

$$E_{sat} = \frac{h\nu \cdot A}{\Gamma\left(dg/dN\right)} \tag{1}$$

where $h\nu$ is the energy of the photons, A is the optical cross-sectional area, Γ is the optical confinement factor and dg/dN is the differential modal gain. Eq. 1 shows that higher gain saturation can be achieved by increasing the modal size, and by reducing the modal confinement and differential gain.

B. Timing jitter

Timing jitter is an intrinsic characteristic of SMLLs, originating mainly from spontaneous emission and carrier fluctuations within the cavity [12]. A decreased coupling of the

amplified spontaneous emission to the guided optical mode results in a narrower RF linewidth and a lower timing jitter [13]. The spontaneous emission coupling factor β_{sp} is related to the number of spontaneously emitted photons coupled to the lasing mode, and is given by [14]:

$$\beta_{sp} = \Gamma_a \frac{r_{sp}}{R_{sp}} \quad (2)$$

where Γ_a is the optical confinement factor of the active layer, r_{sp} is the spontaneous emission coupling rate to the guided mode, and R_{sp} is the total spontaneous emission rate. Eq. 2 shows that β_{sp}, and consequently the timing jitter, decrease with the modal gain overlap Γ_a.

C. Pulsewidth and Chirp

The optical pulses circulating in the cavity of SMLLs are subjected to pulse shaping mechanisms in the gain and saturable absorber sections as a consequence of the interplay between the dynamical variations of gain and absorption in the material. The temporal intensity dependence of the refractive index leads to the nonlinear phenomenon of self-phase modulation (SPM), which modifies the optical spectrum [15]. More precisely, as the gain reaches the saturation level, the carriers coupled to the refractive index through the linewidth enhancement factor (α-factor) induce a phase modulation of the optical pulse, which shifts the optical spectrum towards longer wavelengths and broadens it beyond the Fourier transform limit. At high pulse energy, the temporal pulse broadening and timing jitter are exacerbated by the gain dispersion induced by the group velocity dispersion (GVD) [15]. An opposite effect is triggered by the saturation of the saturable absorber (SA), which operates in a high-carrier density regime, and hence blue-shifts the optical spectrum and provides phase stabilization [10]. The resulting pulse frequency chirp depends on the mutual relationship between the saturation energies in the gain and absorber sections. A simple technique to reduce the pulse chirp is to decrease the broadening in the gain section by increasing its gain saturation level. As previously discussed, high gain saturation is also a requirement for high pulse energy and low timing jitter, and this can be achieved by optimizing the mode size, differential gain and optical confinement factor (see Eqs. 1, 2).

Based on the above discussion, an optimized laser material was designed and verified experimentally. The number of QWs was reduced from five to three in order to decrease the differential gain. Furthermore, a passive far field reduction layer (FRL) was inserted in the lower *n*-type cladding layer to expand the modal spot size [16]. The modal expansion caused by the FRL has two main advantages: first, it decreases the output beam divergence angle and hence improve the coupling to single mode fibers; second, it reduces the confinement factor Γ and therefore decreases the spontaneous emission coupling factor and further increases the saturation energy. The structure consists of a 1.8 μm thick *n*-doped InP buffer layer, a 160 nm thick 1.1Q FRL, a 0.75 μm thick *n*-doped InP spacer layer, a 10 nm thick graded-composition AlGaInAs layer with Al content increasing from 0.404 to 0.423, an *n*-doped AlGaInAs cladding layer (60 nm), and a 60nm thick graded-index separate confinement heterostructure (GRINSCH) AlGaInAs layer with Al composition decreasing from 0.423 to 0.338. The active region has three 6 nm thick compressive-strained (+1.2%) AlGaInAs QWs and four 10nm thick tensile-strained (−0.3%) AlGaInAs barriers. The upper cladding above the active layer is formed by another 60nm thick GRINSCH AlGaInAs layer with Al composition changing from 0.338 to 0.423, a 60 nm thick *p*-doped AlGaInAs cladding layer, a 50 nm *p*-doped InP, a 20nm thick $In_{0.85}Ga_{0.15}As_{0.33}P_{0.67}$ (1.1Q), a 1.6 μm thick *p*-doped InP cladding layer, a 50 nm thick layer of $In_{0.71}GaAs_{0.62}P$ (1.3Q) and finally a 0.2 μm thick *p*+-doped InGaAs contact layer.

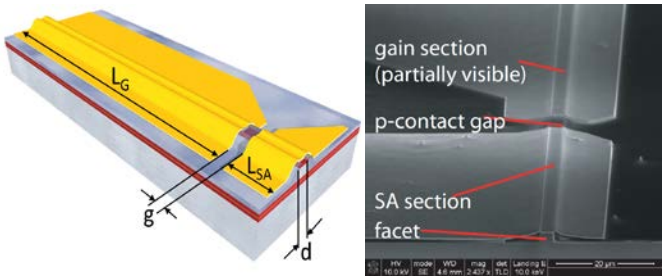

Fig. 1. Schematic diagram (left) and SEM image (right) of the devices.

SMLLs were fabricated with standard lithographic, dry etching, planarization and metallization techniques [17] on both the standard 5 QW and optimized 3 QW epi-layer designs. A schematic diagram showing the devices layout and an SEM image of the examined MLLs are presented in Fig. 1. The devices were designed to operate with a sub-40 GHz repetition rate. The total cavity length of 1136 μm and 1256 μm was defined by the chip cleaving and resulted in a fundamental repetition rate of 38.8 GHz and 35.1 GHz for the 5 QW and 3 QW devices, respectively. The devices reported in this work have SA lengths corresponding to 3.5 % of the total cavity length of the lasers, which produced the best ML performance (narrow and stable pulses over the greatest range of gain currents and SA voltages). The absorber section was placed next to one of the facets and the electrical isolation between the gain and the SA sections was realized by a 10 μm wide gap between the *p*-type metal contacts. Passive mode locking was obtained by forward biasing and reverse biasing the gain and absorber regions, respectively.

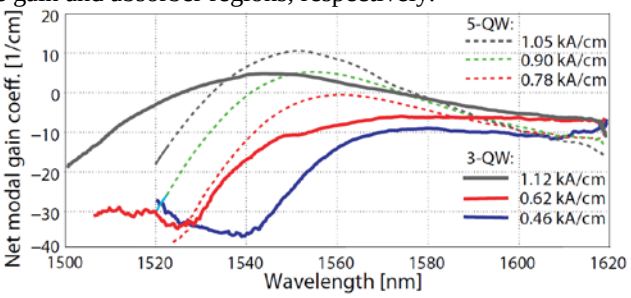

Fig. 2. Modal gain coefficient spectrum of the active materials at different current density levels, obtained with the Hakki-Paoli technique.

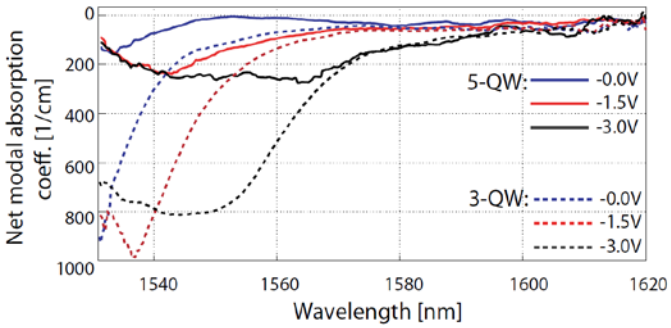

Fig. 3. Modal absorption coefficient spectrum of the active materials at different saturable absorbers biasing levels, obtained with the Hakki-Paoli technique.

III. Experimental Results

A. Gain and Absorption Characteristics

Gain and loss measurements were first performed to evaluate the effects of the introduced material modifications on parameters such as the material loss coefficient, threshold current density and gain peak wavelength. The results of the gain characterization in Fig. 2 show the modal gain coefficient spectra of the dominant transverse electric (TE) component for different injected current values for 5 QW and 3 QW devices. The standard material demonstrates positive gain coefficient values at a current density of 0.78 kA/cm^2, compared to the ~1 kA/cm^2 for the modified structure. The 3QW structure has a lower gain peak that the 5QW structure at current densities above 1 kA/cm^2, which results from its lower confinement factor. This feature gives weaker gain dispersion, and, through the α-factor, lowers the group-velocity dispersion (GVD). The modal gain and absorption coefficient spectra were used to evaluate both the internal losses and differential gain of the materials [18], which gave values of ~20 cm^{-1} and ~5 × 10^{-17} cm^2 for the 5 QW design, and ~8 cm^{-1} and 2.7 × 10^{-17} cm^2 for the 3 QW design. These figures were confirmed through the characterization of broad area lasers with varying cavity lengths [19, 20]. The reduction in the differential gain is a consequence of the reduction in the number of QWs, while the lower optical losses are caused by the reduced optical interaction with the highly lossy *p*-type doped cladding.

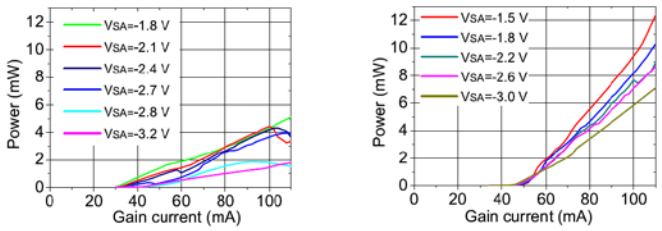

Fig. 4. LI curves for the 5 QW devices (left) compared with LI curves for the 3 QW devices (right).

A comparison of the LI curves, for both 3 QW and 5 QW devices, is shown in Fig. 4. The lasing threshold in the standard material is lower (~30mA) than that presented by the new epi-layer structure (~50mA) consistently with the outcome of the gain measurements. The slope efficiency improves substantially from 0.14 W/A to 0.21 W/A at V_{SA} = 0 V, as expected from the reduction in the internal losses [21].

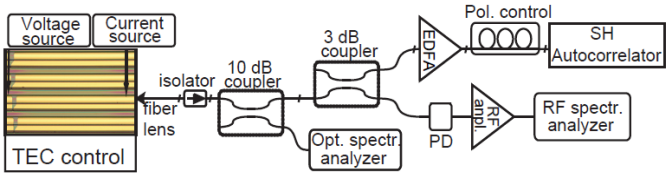

Fig. 5. Experimental set-up for basic characterization of the SMLLs.

B. Characterization of the SMLLs

The experimental set-up used for the basic characterization of the mode-locking of the devices is presented in Fig. 5. The backside temperature of the laser sub-mount is controlled using a Peltier cell, and kept at the temperature of 20 ºC. The light emitted from the facet is coupled into an AR-coated lensed fiber, connected to a fiber pigtailed isolator. The optical signal is simultaneously distributed to an intensity autocorrelator (IAC), an Optical Spectrum Analyzer (OSA) and a Radio Frequency (RF) analyzer (45 %, 10 % and 45 % of the total power, respectively). The electrical signal of the 45 GHz photodiode (PD) is amplified with an RF amplifier (27 dB of gain), while the optical signal is amplified using an Erbium-doped Fiber Amplifier (EDFA), with 15 dB of gain. IAC measurements are performed with a Femtochrome background-free intensity autocorrelator. The whole measurement apparatus is remotely controlled with a PC, allowing for automatic and simultaneous acquisition of all the SMLL parameters.

The dynamical behavior of the devices was characterized for a range of gain section currents (I_g) and SA reverse voltages (V_{SA}) values. In order to create a comprehensive overview of the ML operation, a number of operational parameters were monitored. These included the output power, the Full Width at Half Maximum (FWHM), intensity, and peak-to-pedestal ratio of the Second Harmonic Generation (SHG) intensity autocorrelation, the optical spectrum (peak wavelength, FWHM and modulation depth), the time-bandwidth product (TBP) between the optical spectrum and the non-deconvolved IAC pulsewidth, the RF spectrum (peak frequency, amplitude and FWHM around the fundamental repetition frequency, as well as low frequency components below 5 GHz).

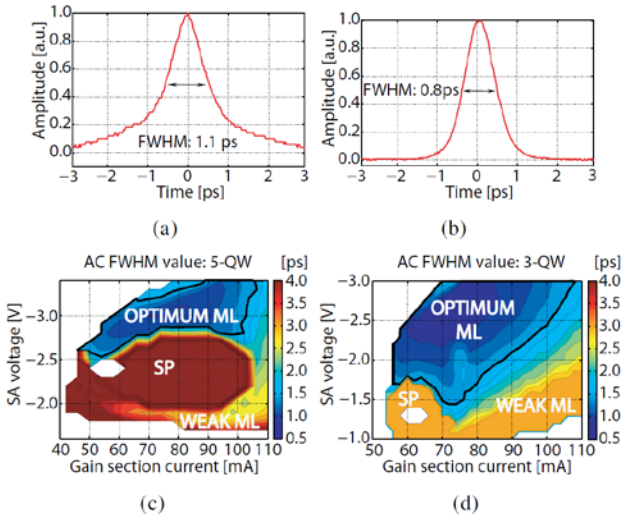

Fig. 6. (a,b) Narrowest intensity autocorrelation traces and (c,d) parametric maps of the IAC FWHM for the 5 QW and 3 QW designs. The black contour line in (c) & (d) shows the limit of the biasing region in which the pulse FWHM < 1.5 ps.

The comparison of the intensity autocorrelation traces (see Fig. 6 (a,b)) indicates that the shortest attainable pulse decreases from 1.1ps for the 5 QW material to 0.8 ps for the improved design. The maps of the IAC pulsewidth as a function of the laser biasing parameters also show that the 3 QW material generates stable pulses over a much wider range of biasing conditions. In fact, pulses with a FWHM of less than 1.5 ps (black line in Fig. 6 (c, d)) occur over an interval of SA voltages and currents as wide as -1.4 V to -3 V and 55 to 100 mA, respectively. It is also worth mentioning that the 3 QW material requires a lower reverse bias before stable ML is established (-1.4 V as compared to -2.5 V for the 5 QW material).

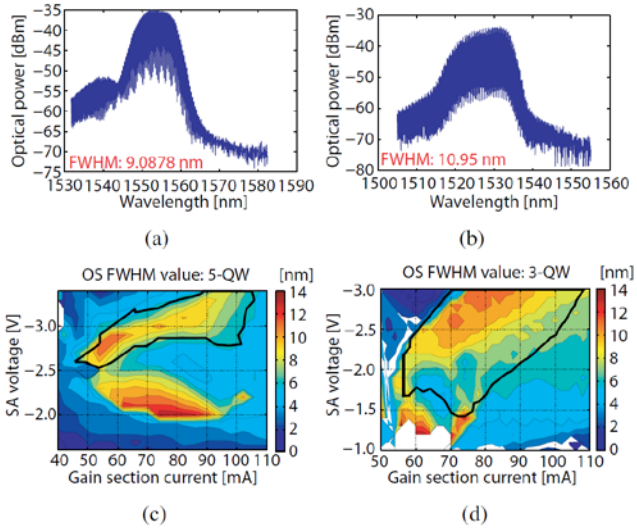

Fig. 7. Optical spectra corresponding to the narrowest IAC pulsewidth (a) for the 5 QW and (b) for the 3 QW device, and parametric color maps of the FWHM of the optical spectrum (c) for the 5 QW and (d) for the 3 QW device. The black contour line in (c) & (d) indicates the limits of the biasing region in which the pulse FWHM < 1.5 ps.

Furthermore, by comparing the areas of the maps outside the optimum ML region, it can be seen that the 3 QW devices are less affected by the self-pulsation (SP) phenomenon, which only arises for low gain currents and SA reverse biases.

The optical spectra for both the 3 QW and the 5 QW SMLLs are juxtaposed in Fig. 7, together with the parametric maps displaying the FWHM of the spectra. With regards to the optical spectrum, stable ML is generally characterized by a symmetrical, single-lobed trace with a comb modulation depth greater than 10 dB and a FWHM ranging between 4 nm and 12 nm. A general feature on the spectra for the 3 QW devices is the absence of the short wavelength side-lobe that is present in the spectra of the 5 QW devices. The maximum FWHM of the optical spectrum within the optimum ML region is approximately 9 nm in the 5 QW case, whereas it extends to 11 nm for the 3 QW devices. Moreover, the 3 QW material shows a much wider range of gain currents over which the FWHM is greater than 10 nm (see fig. 7 (c, d)).

The product between the IAC pulsewidth and the FWHM of the optical spectrum yields the time-bandwidth-product (TBP) of the emitted pulses. To avoid any assumption on the shape of the pulses emitted by the SMLLs, the non-deconvolved pulsewidths directly obtained from the IAC trace were used, which yields a minimum measured TBP of 0.485. If a sech^2 shape was assumed, which was found to be a better fit than a Gaussian envelope, the TBP of a transform-limited pulse would be 0.315. TBP larger than the transform-limited value are the consequence of chirp on the emitted pulses or intensity substructures in their temporal envelopes. The parametric maps of the TBP of the pulses are shown in Fig. 8, both for the 5 QW and 3 QW devices.

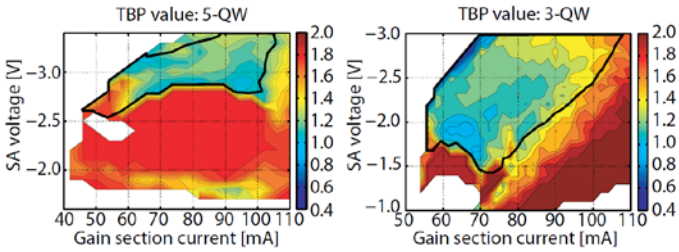

Fig. 8. Parametric maps of the non-deconvolved time bandwidth product (TBP) values. The black contour line in (c) & (d) show the limits of the biasing region in which the pulse FWHM < 1.5 ps.

Despite the fact that none of the measured pulses were transform-limited, once again a definite improvement can be clearly seen for the 3 QW device, whose minimum TBP was 0.8 compared to a minimum value of 1.1 for the 5 QW SMLL. Moreover, the 3 QW material produced a consistently lower TBP across a much wider range of currents and voltages as shown in the colour maps in Fig. 8. This is a first indication that the epitaxial optimization of the laser structure reduces the pulse broadening, producing optical pulses which exhibit lower optical chirp and parasitic temporal substructure.

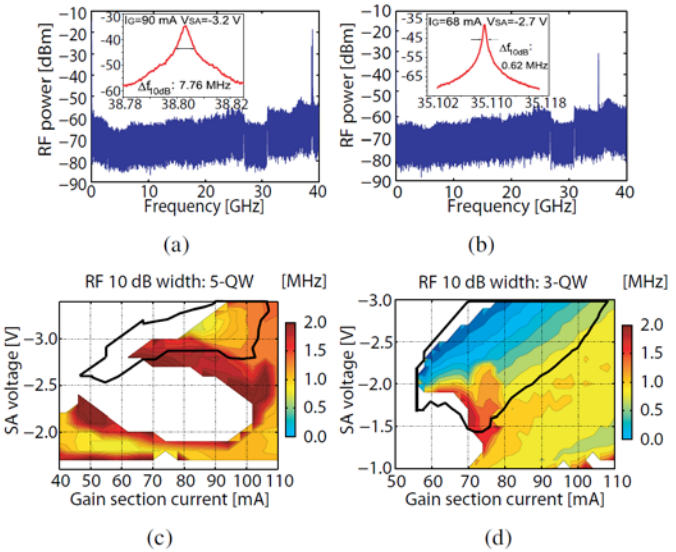

Fig. 9. (a,b) RF spectra corresponding to the narrowest pulsewidth and (c,d) parametric maps of the RF signal 10 dB width for the 5 QW and 3 QW material, respectively. The black contour line in (c) & (d) show the limits of the biasing region in which the pulse FWHM is < 1.5 ps.

The reduction of the timing jitter in the 3QW lasers was confirmed by the analysis of the RF spectra on both material platforms. For the 5QW material, the RF 10 dB linewidth value varies between 1 MHz and 30 MHz in the optimum ML region. Fig. 9 (a) shows the RF spectrum for the narrowest pulse emitted by the 5QW device; which gives a 10 dB RF linewidth value of 7.76 MHz. In general, there was no discernable correlation between the parameter ranges producing the narrowest pulsewidth and those producing the best RF linewidth. The narrowest RF signals are found for currents close to threshold, with the RF line broadening as the current is increased. It is worth noting that values below 100 kHz have been recorded for high gain pumping above three times the laser current threshold, where multimode dynamics sometimes lead to the generation of high-intensity and narrow-linewidth RF peaks. However, these narrow RF lines are the result of incomplete mode-locking that manifests itself with the presence of a pedestal in the time domain and a slow amplitude modulation with a periodicity dictated by the relaxation oscillations. Similarly, for the 3 QW SMLLs the narrowest 10 dB RF linewidth does not correspond to the narrowest pulse, which produces an RF signal with a 620 kHz 10 dB linewidth, shown in Fig. 9 (b). When compared to the 5 QW lasers, the RF 10 dB linewidth values of the 3 QW devices are smaller over a much wider range of currents and voltages indicating improved performance (see Fig. 9 (c) and (d)).

C. Chirp Measurements

The pulse intensity and phase profile have been obtained with the sonogram technique, as described in [22]. The sonogram trace is a time-frequency representation of the optical pulse, of which it measures the arrival time of successive pulse spectral slices, i.e. the group delay (GD). The analysis of the GD evolution with respect to the wavelength can provide useful information about the optical chirp affecting the pulses.

An example of a measurement taken for a 5 QW device is displayed in Fig. 10, where two sonogram traces and the corresponding retrieved temporal intensity and phase profiles are compared for the laser operating under optimum mode-locking conditions (I_G=70 mA) and for the laser driven at high gain current (I_G =110 mA).

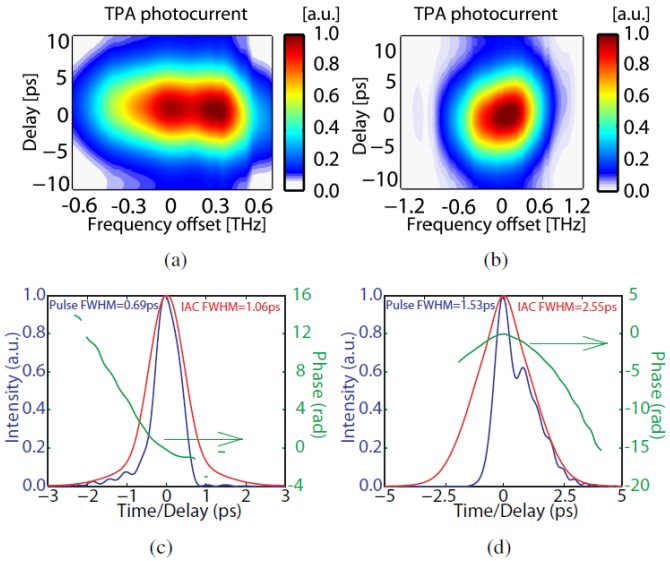

Fig. 10. (a,b) Sonogram and (c,d) temporal traces of the 5 QW device biased at gain currents of 70mA and 110mA, with V_{SA}=-2.8 V.

The effect of non-optimal biasing is clearly visible in the pulse temporal characteristics. Not only does the FWHM of the pulse increase from 0.69 ps to 1.53 ps, but the pulse also presents trailing edge sub-structures. It is worth mentioning that these details would be completely inaccessible through standard measurements of the pulse optical spectrum or of the IAC. In fact, an estimation of the temporal pulse width based only on IAC measurements would require an assumption on the pulse shape and lead to incorrect results, since both the shape and the sub-structure of the pulse change with the biasing conditions. The deconvolution factor, i.e. the ratio between the FWHM values from the IAC and those of the retrieved pulse, for the analyzed 5 QW device of Fig. 10 was found to vary between 1.22 and 2.14.

The results obtained for the 3 QW devices are shown in Fig. 11, again comparing the traces obtained for mode locking under optimal bias conditions and for high gain pumping. The effect of non-optimum biasing is visible through the broadening of the pulse, although the effect is not as pronounced as it was for the 5 QW devices, given the absence of substructures in the trailing edge of the pulse.

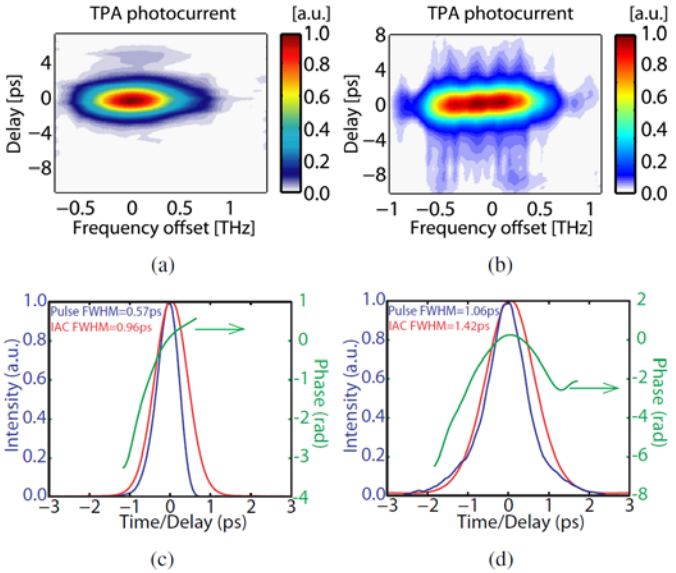

Fig. 11. (a,b) Sonogram and (c,d) temporal traces of the 3 QW device biased at gain currents of 70mA and 110mA, with V_{SA}=-2.4 V.

The minimum recorded pulse width was 0.57 ps for the 3 QW device, against 0.69 ps obtained for the 5 QW. As a general trend, it was found that the temporal profile of pulses obtained from 3 QW devices is more smooth and symmetric than for the pulses emitted from 5 QW devices, and the deconvolution factor for the best pulses has a value of 1.64, close to the value associated with an ideal $sech^2$ pulse (1.54).

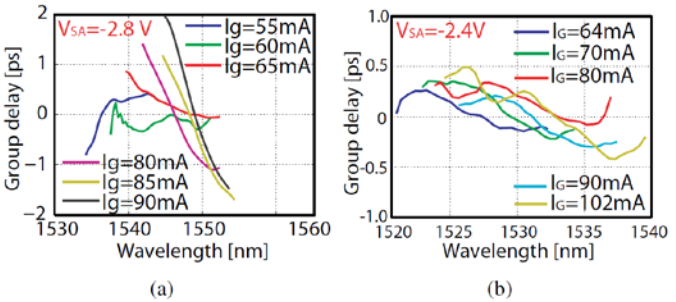

Fig. 12. Group delay profiles of (a) 5 QW and (b) 3 QW MLLs, for different values of gain currents and V_{SA}=-2.8 V and -2.4 V, respectively.

A summary of the chirp measurements across the ML region for both 5 QW and 3 QW device is shown in Fig. 12, where the GD profiles of 5 QW and 3 QW SMLLs are compared for various biasing currents. All devices show a general trend of positive linear chirp in the pulse phase with the chirp being more sensitive to bias variations in the gain section than in the SA. The prevailing positive chirp observed in the characterized SMLLs agrees with previously reported theoretical phase profiles in passively mode-locked semiconductor devices [23, 24]. A clear trend of the 5 QW devices is a pronounced increase of chirp with increasing gain current that is accompanied by the presence of higher order chirp. The 3 QW devices exhibit both a lower and more linear chirp up to bias currents of over two times the threshold. Furthermore, the chirp profile shows very little variations over the biasing parameter region that shows stable ML.

IV. Conclusion

In summary, we have demonstrated how optimization of the epitaxial structure of the laser material can greatly improve the mode-locking performance. Specifically, we have confirmed that reducing the number of QWs and introducing a FRL to expand the optical mode profile lead to an increase in the gain saturation energy and a decrease in both the spontaneous emission coupling factor and internal losses. These modifications have a substantial and positive impact on the peak power, pulsewidth, timing jitter and chirp of the emitted optical pulses. To quantify the benefits of the new design, device performance under ML operation have been assessed and compared to those of SMLLs fabricated on a standard 5 QW laser material. The new design shows an increase in the maximum peak power from ~130 mW to ~250 mW, a decrease in the minimum pulsewidth from 690 fs to 570 fs and from 7.76 MHz to 620 kHz in the RF 10dB linewidth. Of great relevance to applications is also the substantial increase of the biasing parameter region over which the devices fabricated on the new material exhibit stable mode-locking operation. A thorough comparison of the emitted pulses on the two material systems was performed with a sonogram technique, which provided detailed information on the shape of the pulse and evolution of the chirp as a function of the biasing parameters. The increased gain saturation level in the 3 QW design and the subsequent reduction in non-linear effects lead to the formation of more symmetrical pulses with lower chirp. Furthermore, the chirp in the pulses is more linear and much less affected by changes in the gain current.

Acknowledgment

The authors would like to thank the staff of the James Watt Nanofabrication Centre at the University of Glasgow. This research was sponsored by the UK Engineering and Physical Sciences Research Council (project EP/E065112/1).

References

[1] F. Kefelian, S. O'Donoughe, M. Todaro, J. McInerney, and G. Huyet, "RF Linewidth in monolithic Passively Mode-Locked Semiconductor Laser" *IEEE Photonics Technol. Lett.*, vol. 20, no. 16, pp. 1405–64.

[2] C. Brenner, C.-S. Friedrich, and M. Hofmann, "Semiconductor Diode Lasers for Terahertz Technology," *Journal of Infrared, Millimeter and Terahertz Waves*, pp. 1–14, Jul. 2011.

[3] E.A. Avrutin, J.H. Marsh, and E. L. Portnoi, "Monolithic and multi-gigahertz mode-locked semiconductor lasers: constructions, experiments, models and applications", *Optoelectronics, IEE Proceedings*, Vol. 147 no. 4 pp. 251–278, 2000.

[4] K. Yvind, D. Larsson, L.J. Christiansen, C. Angelo, L.K. Oxenlwe, J. Mrk, D. Birkedal, J.M. Hvam, and J. Hanberg, "Low-jitter and high-power 40-ghz all-active mode-locked lasers", *Photonics Technology Letters, IEEE*, vol. 16 no. 4 pp. 975–977, Apr. 2004.

[5] S.V.Kukarin S.V.Smirnov, S.M. Kobtsev and S.K.Turitsyn, "Modelocked fibre lasers with high-energy pulses", in *Laser Systems for Applications*, pp. 39–58, InTech, New York, 2011. Available online: http://www-users.aston.ac.uk/~turitssk/InTech.pdf.

[6] M.S. Stix and E.P. Ippen, "Pulse shaping in passively modelocked ring dye lasers", *Quantum Electronics, IEEE Journal of*, Vol. 19 no. 4, pp. 520–525, Apr. 1983

[7] L. Hou, P. Stolarz, J. Javaloyes, R. Green, C. Ironside, M. Sorel, and A. Bryce, "Subpicosecond pulse generation at quasi-40-ghz using a passively mode-locked AlGaInAs-InP 1.55 μm strained quantum-well

laser," *Photonics Technology Letters, IEEE*, vol. 21, no. 23, pp. 1731–1733, Dec.1, 2009.
[8] G. Mezosi, M.J. Strain, S. Furst, Z. Wang, S. Yu, and M. Sorel. "Unidirectional bistability in AlGaInAs microring and microdisk semiconductor lasers", *Photonics Technology Letters, IEEE*, Vol. 21, no. 2, pp. 88–90, Jan. 2009.
[9] M. Zanola, M.J. Strain, G. Giuliani, and M. Sorel, "Post-growth fabrication of multiple wavelength DFB laser arrays with precise wavelength spacing", *Photonics Technology Letters, IEEE*, Vol. 24 no. 12, pp. 1063–1065, Jun. 2012.
[10] D. Derickson, R. Helkey, A. Mar, J. Karin, J. Wasserbauer, and J. Bowers, "Short pulse generation using multisegment mode-locked semiconductor lasers," *Quantum Electronics, IEEE Journal of*, vol. 28, no. 10, pp. 2186 –2202, Oct. 1992
[11] G. Agrawal and N. Olsson, "Self-phase modulation and spectral broadening of optical pulses in semiconductor laser amplifiers," *Quantum Electronics, IEEE Journal of*, vol. 25, no. 11, pp. 2297 – 2306, Nov. 1989.
[12] K. Yvind, D. Larsson, J. M. rk, J. rn M. Hvam, M. Thompson, R. Penty, and I. White, "Low-noise monolithic mode-locked semiconductor lasers through low-dimensional structures," *A. A. Belyanin and P. M. Smowton, Eds.*, vol. 6909, no. 1. SPIE, 2008, p. 69090A. Available online: http://link.aip.org/link/?PSI/6909/69090A/1
[13] K. Merghem, A. Akrout, A. Martinez, G. Moreau, J.-P. Tourrenc, F. Lelarge, F. V. Dijk, G.-H. Duan, G. Aubin, and A. Ramdane, "Short pulse generation using a passively mode locked single InGaAsP/InP quantum well laser," Opt. Express, vol. 16, no. 14, pp. 10 675–10 683, Jul 2008. Available online: http://www.opticsexpress.org/abstract.cfm?URI=oe-16-14-10675
[14] T. Numai, "Fundamentals of Semiconductor Lasers", New York: *Springer*, 2004.
[15] G. Agrawal, "Effect of gain dispersion on ultrashort pulse amplification in semiconductor laser amplifiers," *Quantum Electronics, IEEE Journal of*, vol. 27, no. 6, pp. 1843 –1849, Jun. 1991.
[16] L. Hou, M. Haji, J. Akbar, B. Qiu, and A. C. Bryce, "Low divergence angle and low jitter 40 GHz AlGaInAs/InP 1.55 μm mode locked lasers", Opt. Lett., vol. 36, no. 6, pp. 966–968, Mar. 2011. Available online: http://ol.osa.org/abstract.cfm?URI=ol-36-6-966
[17] L. Hou, P. Stolarz, J. Javaloyes, R. Green, C. Ironside, M. Sorel, and A. Bryce, "Subpicosecond Pulse Generation at Quasi-40-GHz Using a Passively Mode-Locked AlGaInAs-InP 1.55 μm Strained Quantum-Well Laser," IEEE Photonics Technol. Lett., vol. 21, no. 23, pp. 1731–1733, Dec. 2009.
[18] B. W. Hakki and T. L. Paoli, "Gain spectra in GaAs double−heterostructure injection lasers", *Journal of Applied Physics*, vol. 46, pp. 1299–1306, 1975.
[19] S. D. McDougall and C. N.; Ironside, "Measurements of reverse and forward bias absorption and gain spectra in semiconductor laser material," Electronics Letters , vol.31, no.25, pp.2179–2181, 7 Dec 1995
[20] J. D. Thomson, H. D. Summers, P. J. Hulyer, P. M. Smowton, and P. Blood, "Determination of single-pass optical gain and internal loss using a multisection device", *Applied Physics Letters*, vol. 75, pp. 2527–2529 (1999).
[21] J. Piprek, P. Abraham, and J. E. Bowers, "Cavity length effects on internal loss and quantum efficiency of multiquantum-well lasers," *Selected Topics in Quantum Electronics, IEEE Journal of* , vol.5, no.3, pp.643–647, May/Jun 1999
[22] P. Stolarz, G. Mezosi, M.J. Strain, A.C. Bryce, and M. Sorel, "Highly Sensitive Sonogram for Assessment of Chirp in Semiconductor Mode-Locked Lasers", *Quantum Electronics, IEEE Journal of*, vol. 48, no. 8, pp. 995 –1003, Aug. 2012.
[23] K. A. Williams, M. G. Thompson, and I. H. White, "Long-wavelength monolithic mode-locked diode lasers," *New Journal of Physics*, vol. 6, no. 1, p. 179, 2004.
[24] M. Schell, M. Tsuchiya, and T. Kamiya, "Chirp and stability of modelocked semiconductor lasers," *IEEE J. Quantum Electron.*, vol. 32, no. 7, pp. 1180–1190, Jul. 1996.

Piotr M. Stolarz received the Ph.D. degree in the School of Engineering at the University of Glasgow in 2012. He received the M.Sc. degree in electronics and electrical engineering from the University of Glasgow, Glasgow, U.K., and the M.Sc. degree in electrical engineering from Lublin University of Technology, Lublin, Poland, in 2007 and 2008, respectively. His current research interests include semiconductor mode-locked lasers and measurement techniques for the characterization of ultrashort pulses.

Vincenzo Pusino received the Ph.D. degree in the School of Engineering at the University of Glasgow in 2014. He received the M. Sc. Degree in electronics and electrical engineering from the University of Pavia in 2008. He is now a Research Assistant at the University of Glasgow. His research interests include semiconductor mode-locked lasers, nonlinear integrated optics and mid-IR detectors.

Jehan Akbar received the Ph.D. degree in the School of Engineering at the University of Glasgow in 2012. He is currently a lecture within the Physics Department at Hazara University in Pakistan. His research interests include semiconductor mode-locked lasers and high-power monolithic semiconductor amplifiers.

Gábor Mezősi graduated in electronics engineering at the Budapest University of Technology and Economics, Budapest, Hungary in 2005. He received the Ph.D. degree in semiconductor ring lasers from University of Glasgow, Glasgow, U.K. in 2010. His research activities include semiconductor ring lasers, integrated high power lasers, mode-locked lasers and VCSELs.

Lianping Hou was born in Hunan, China, in 1969. He received the B.Eng. degree from the Central South University of technology, Changsha, China, in 1992, the M.A. degree from Huazhong University of Science and technology, Wuhan, China, in 2003, and the Ph.D. degree from the Chinese Academy of Sciences, Beijing, China, in 2005. He worked as a Postdoctoral Researcher in the Semiconductor Photonics Group at the Trinity College in Dublin, Ireland from 2006, and then as a Research Associate at the University of Bristol. He is currently a Research Fellow at the University of Glasgow. His research interests include III-V semiconductor lasers, optoelectronic components and photonic integrated circuits.

A. Catrina Coleman was born in 1956 and educated in physics at the University of Glasgow, receiving her Ph.D. degree in 1987. She joined the optoelectronics group of the Department of Electronics and Electrical Engineering at Glasgow as a post-doctoral Research Assistant, and was appointed a Research Fellow in 1992, becoming a Senoir research Fellow in 1997 and Professorial Research Fellow in 2005. In 2012 she took up a position as a professor at the University of Illinois at Urbana-Champaign, working in the Micro and Nanotechnology Lab. Her research interests include photonic integration, mode-locked laser diodes and high power semiconductor lasers.

Anthony E. Kelly received the B. Sc., M.Sc., and Ph. D. degrees from the University of Strathclyde, Glasgow, U. K. He was with the British Telecom Laboratories and Corning. He was also a Co-Founder of Kamelian Ltd., Oxforshire, U. K., and Amphotonix Ltd., Glasgow. He is currently with the School of Engineering, University of Glasgow. He has authored or co-authored more than 150 journal and conference papers on a range of optoelectronic devices and systems and holds a number of patents. His current research interests include semiconductor optical amplifiers and related devices, visible light communications using GaN devices, and high speed lasers for PON systems.

Marc Sorel received the Electronics Engineering and the Ph.D. degree from the Università di Pavia, Pavia, Italy, in 1995 and 1999, respectively. in 1998, he joined the Optoelectronics Group at the University of Glasgow, where he holds a senior lectureship position. His research interests include semiconductor technologies for monolithic and hybrid integration.